Significant reduction in the thermal conductivity of Si-substituted Fe_2VAl epilayers

K. Kudo,[1] S. Yamada,[1,2,*] J. Chikada,[1] Y. Shimanuki,[1] T. Ishibe,[1] S. Abo,[1] H. Miyazaki,[3] Y. Nishino,[3] Y. Nakamura,[1] and K. Hamaya[1,2,†]

[1]*Graduate School of Engineering Science, Osaka University, 1-3 Machikaneyama, Toyonaka 560-8531, Japan*
[2]*Center for Spintronics Research Network, Graduate School of Engineering Science, Osaka University, 1-3 Machikaneyama, Toyonaka 560-8531, Japan*
[3]*Department of Physical Science and Engineering, Nagoya Institute of Technology, Nagoya 466-8555, Japan*

(Received 18 November 2018; published 1 February 2019)

We experimentally find that the substitution of Si for Al in Heusler-type Fe_2VAl epilayers contributes to the significant reduction in the thermal conductivity, in which Fe_2VAl is one of the next-generation thermoelectric materials without using toxic elements. Because of the low-temperature growth of the epilayers, the Si substitution induces the decrease in the degree of $L2_1$ ordering, giving rise to the formation of V-Si antisite defects in the epilayers. For $Fe_2VAl_{0.57}Si_{0.43}$ epilayers, we can obtain a low thermal conductivity of $\sim$3.9 W/(m K), one-third less than Si-substituted Fe_2VAl bulk samples [Lue *et al.*, Phys. Rev. B **75**, 064204 (2007)]. We discuss that a possible origin of the low thermal conductivity is related to the low lattice thermal conductivity due to the presence of the V-Si antisite defects.

DOI: 10.1103/PhysRevB.99.054201

I. INTRODUCTION

Thermal conductivity (κ) is one of the key physical parameters in developing thermoelectric materials, which enable the conversion between thermal and electrical energy [1–4]. The κ value for ordinary metals and semimetals comes generally from the contributions due to electrons/holes carrier transporting heat (κ_c) and phonons traveling via the lattice (κ_{ph}) [1,3,5], where κ_c can be roughly estimated from the resistivity (ρ) by using the Wiedemann-Franz law above Debye temperature [1,5,6] and κ_{ph} is roughly approximated by $\kappa_{ph} = Cvl/3$ [5,7,8], where C, v, and l are lattice specific heat, group velocity, and mean-free pass of phonons, respectively. In the field of thermoelectric conversion, low κ values are required to demonstrate high-performance thermoelectric materials and devices [1–4].

In general, a low value of κ_c can be obtained by tuning the carrier concentration in thermoelectric materials [1]. As methods for reducing the value of κ_{ph}, on the other hand, heavy element substitutions [9–12] and introducing nanostructures [1–4,13–18], suppressing v and l, respectively, have been utilized. Actually, thin-film superlattice structures [1,17,18], connected Si nanocrystals [15], and randomly embedded quantum dots [1,13] have achieved very low κ_{ph} values. The other approach is introducing atomic disorder, which can increase the mass-disorder-induced and/or anharmonic scattering of phonons, leading to the reduction of l [1,5,19]. In regard to these, the experimental demonstrations have been reported in well-known thermoelectric materials such as bismuth telluride (Bi-Te), silicon-germanium (Si-Ge), and lead-telluride (Pb-Te) compounds [1,20–23].

*yamada@ee.es.osaka-u.ac.jp
†hamaya@ee.es.osaka-u.ac.jp

As a next-generation thermoelectric material to replace Bi-Te compounds from the viewpoint of not containing toxic elements, $L2_1$-ordered Fe_2VAl [24], a full-Heusler semimetallic alloy, has been reported. Many theoretical [25–32] and experimental [33–35] studies have so far supported the presence of a sharp pseudogap near the Fermi level (E_F) in the electronic band structure. This means that the electrical and thermoelectric properties such as electrical resistivity (ρ) and Seebeck coefficient (S) can be modulated by changing the electronic band structure or shifting E_F because the value of S in metallic systems is proportional to the gradient and reciprocal for the density of states (DOS) at E_F [36]. Actually, for bulk and thin-film Fe_2VAl samples, the reduction in ρ and the enhancement in $|S|$ with maintaining the pseudogap structure near E_F have been demonstrated by changing the chemical composition [10,37–41] or substituting constituent elements [12,41–46]. As a result, the value of κ of the polycrystalline $Fe_2VTa_{0.05}Al_{0.95}$ processed by high-pressure torsion reached $\sim$5 W/(m K) at 300 K [46], comparable with Bi-Te compounds [$\kappa \sim 1.5$ W/(m K)] [1].

Recently, we achieved a perfectly stoichiometric Fe_2VAl epilayer by using a nonstoichiometric molecular beam epitaxy (MBE) growth technique at a low growth temperature of 350 °C [47]. We found that the low-temperature grown Fe_2VAl epilayers have a relatively low κ value [$\sim$7.5 W/(m K) [47]], compared to Fe_2VAl bulk [$\sim$28 W/(m K) [44]], despite almost no reduction in S. In addition, because the grown Fe_2VAl epilayers included the $L2_1$-ordered structure and the κ value did not change with decrease of film thickness [47], we judged that the small κ value is not caused by introducing the grain boundaries and the low-dimensional structures. From these experimental data, we speculated that the atomic-level disordered structures such as point defects in the low-temperature grown Fe_2VAl epilayers result in the scattering of phonons. However, the

©2019 American Physical Society

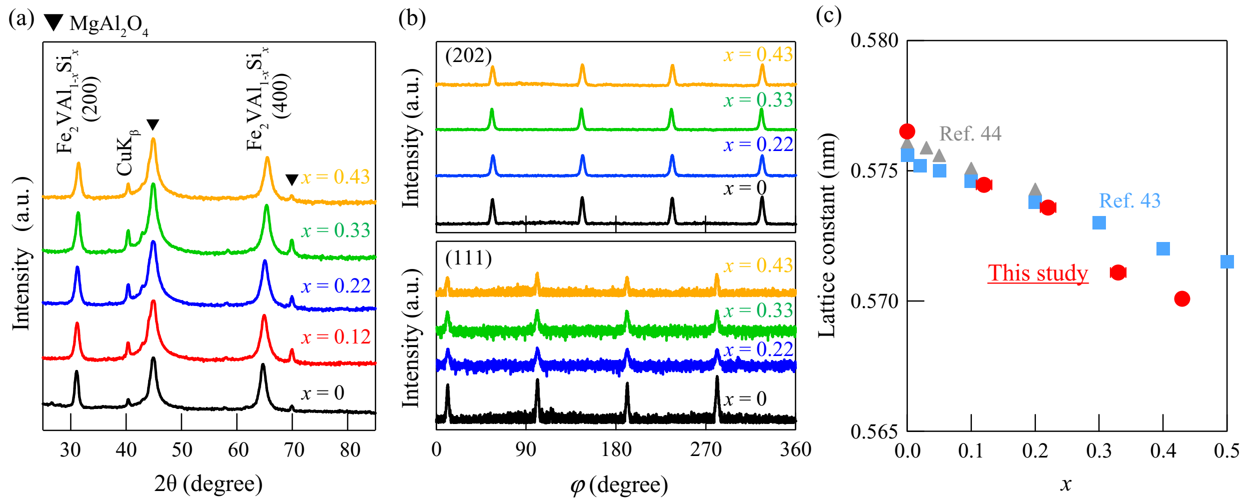

FIG. 1. (a) θ-2θ XRD patterns for the $Fe_2VAl_{1-x}Si_x$ epilayers. (b) ϕ-scan measurements of (202) and (111) plane for the $Fe_2VAl_{1-x}Si_x$ epilayers. (c) The lattice constant of the $Fe_2VAl_{1-x}Si_x$ epilayers estimated from the Fig. 1(a), together with those for the bulks [43,44].

correlation between the atomic-level disorder and the small κ value in the Fe_2VAl Heusler alloy has not been discussed yet.

In this paper, we experimentally study the influence of the substitution of Si for Al in the MBE-grown Fe_2VAl epilayers on the value of κ. Because of the low-temperature growth, we found that the Si substitution induces the decrease in the degree of $L2_1$ ordering. From the first-principles calculations, the electrical properties of the $Fe_2VAl_{1-x}Si_x$ epilayers can be understood by considering the presence of the V-Si antisite defects. For $Fe_2VAl_{0.57}Si_{0.43}$ epilayers, we can obtain a low thermal conductivity of $\sim$3.9 W/(m K), one-third less than Si-substituted Fe_2VAl bulk samples [43]. A possible origin of the low thermal conductivity is discussed as a consequence of the low lattice thermal conductivity due to the presence of the V-Si antisite defects in the Si-substituted Fe_2VAl epilayers.

II. RESULTS

A. Epitaxial growth and structural characterization

Si-substituted Fe_2VAl ($Fe_2VAl_{1-x}Si_x$) epilayers with thicknesses of 50–150 nm were grown on $MgAl_2O_4$(100) substrates (sample size: 1 × 1 cm^2) by using an MBE technique with nonstoichiometric deposition [47–52]. As the mismatch between the lattice constant of $Fe_2VAl_{1-x}Si_x$ polycrystalline bulks (0.576–0.572 nm) [43,44] and a half of diagonal length of the lattice constant of $MgAl_2O_4$ ($1/\sqrt{2}$ × 0.8083 nm = 0.5715 nm) is less than 1%, high-quality epitaxial growth of the $Fe_2VAl_{1-x}Si_x$ layers can be expected [47]. After loading the $MgAl_2O_4$(100) substrates into the MBE chamber with a base pressure of $\sim 10^{-7}$ Pa, the heat treatment at 600 °C for 1 h was performed. From *in situ* reflection high-energy electron diffraction (RHEED) observations (not shown here), the good surface flatness of the $MgAl_2O_4$(100) substrates was confirmed. Cooling the substrate temperature down to 350 °C, we grew $Fe_2VAl_{1-x}Si_x$ layers by co-evaporating Fe, V, Al, and Si using Knudsen cells. Here we set the supplied atomic composition ratio of Fe : V : Al : Si to 1.8 : 1.2 : 2(1-x) : x during the growth. The chemical composition of the grown layers was estimated using the results of energy dispersive x-ray spectroscopy (EDX). The estimated errors for each x are shown by error bars in Figs. 1(c), 3, and 4(a).

From the RHEED observations, good two-dimensional epitaxial growth was guaranteed for all the $Fe_2VAl_{1-x}Si_x$ layers (not shown here). After the growth, structural characterizations of the grown $Fe_2VAl_{1-x}Si_x$ epilayers were carried out. Figure 1(a) shows the θ-2θ x-ray diffraction (XRD) patterns for the $Fe_2VAl_{1-x}Si_x$ epilayers in $0 \leqslant x \leqslant 0.43$. Except for the peaks derived from the $MgAl_2O_4$ substrate, only the (200) and (400) diffraction peaks are clearly seen at 2θ values of $\sim 31^\circ$ and $\sim 65^\circ$, respectively, indicating the formation of (100)-oriented $Fe_2VAl_{1-x}Si_x$ epilayers. The ϕ-scan measurements for various x are presented in Fig. 1(b). For all the epilayers, (202) diffraction peaks with fourfold symmetry are seen, indicating the in-plane crystal orientation of Fe_2VAl[100](100)//$MgAl_2O_4$[110](100). The (111) diffraction peaks meaning the presence of the $L2_1$-ordered structure are also observed but the intensity of the (111) diffraction peaks for the Si-substituted epilayers is relatively decreased compared to that for the nonsubstituted epilayer. This feature implies that the substitution of Si for Al causes the decrease in the degree of $L2_1$ ordering in the $Fe_2VAl_{1-x}Si_x$ epilayers. We can also estimate the lattice constant of the $Fe_2VAl_{1-x}Si_x$ epilayers from the XRD data in Fig. 1(a) and summarize the lattice constant as a function of x, together with those for $Fe_2VAl_{1-x}Si_x$ polycrystalline bulks reported previously [43,44], in Fig. 1(c). For both $Fe_2VAl_{1-x}Si_x$ epilayers and bulks, the lattice constant decreases almost linearly following the size of the atomic radius of Al and Si (Al > Si) with increasing x. This feature indicates that the change in the lattice constant according to the conventional Vegard's law can be seen even for the low-temperature grown $Fe_2VAl_{1-x}Si_x$ epilayers.

Further structural investigations were carried out by cross-sectional transmission electron microscopy (TEM) and high-angle annular dark-field scanning transmission electron microscopy (HAADF-STEM). A typical HAADF-STEM image of the $Fe_2VAl_{0.57}Si_{0.43}$ epilayer is shown in Fig. 2. The $Fe_2VAl_{0.57}Si_{0.43}$ epilayer on $MgAl_2O_4$(100) is uniformly

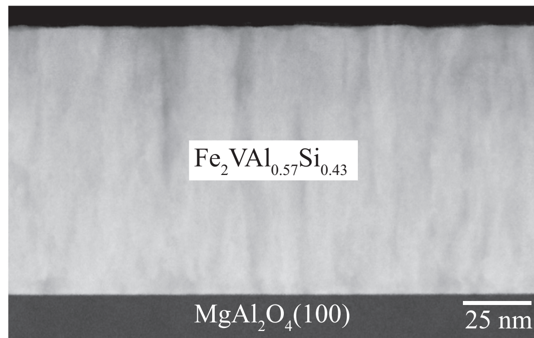

FIG. 2. HAADF-STEM image of $Fe_2VAl_{0.57}Si_{0.43}/MgAl_2O_4(100)$.

grown although there are some dislocations in the epilayer along [001], similar to the stoichiometric Fe_2VAl epilayer previously shown in Ref. [47]. The contrast of the HAADF image in Fig. 2 is nearly homogeneous over the measured area. These features are also similar to those in the stoichiometric Fe_2VAl epilayer [47]. Thus, although the substitution of Si for Al does not largely deteriorate the quality of the $Fe_2VAl_{1-x}Si_x$ epilayer, it can only induce the decrease in the degree of $L2_1$ ordering.

B. Electrical properties and electronic band structures

To understand the impact of the decrease in the degree of $L2_1$ ordering on the electronic band structure in Si substituted Fe_2VAl epilayers, we first examined electrical properties with changing x. For evaluating transport properties, the $Fe_2VAl_{1-x}Si_x$ epilayers were patterned into Hall-bar devices with $80 \times 80\ \mu m^2$ in size, as shown in the inset of Fig. 3, by conventional photolithography and Ar ion milling [47]. Figure 3 shows the values of ρ at 300 K as a function of x in the $Fe_2VAl_{1-x}Si_x$ epilayers, together with those in polycrystalline bulks in Refs. [43,44]. Here the temperature dependence of ρ for various x is presented in the Supplemental Material (Fig. S1) [53]. The value of ρ at 300 K in the epilayer is decreased with increasing x, together with a small change in ρ at $x =$ 0.12 and 0.22. Whereas the decrease in ρ with increasing x is consistent with that in the bulks in Refs. [43,44], the value of ρ in the epilayer is always larger than that in the bulk in all x. Considering the structural characterizations in Figs. 1 and 2, we can interpret that the increase in ρ is related to the decrease in the degree of $L2_1$ ordering, which leads to the carrier scattering in the $Fe_2VAl_{1-x}Si_x$ epilayers.

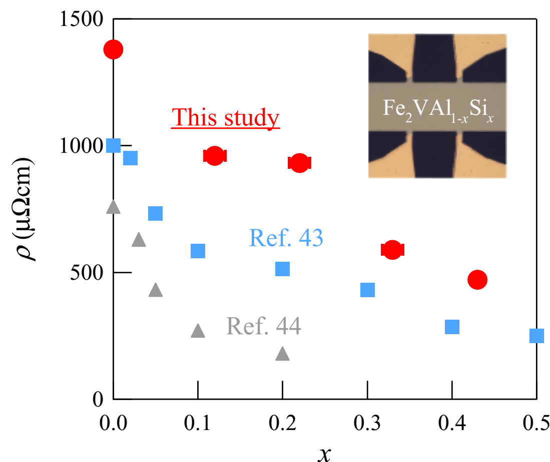

FIG. 3. The values of ρ at 300 K as a function of x in the $Fe_2VAl_{1-x}Si_x$ epilayers and bulks in Refs. [43,44]. The inset shows an optical micrograph of a fabricated Hall-bar device.

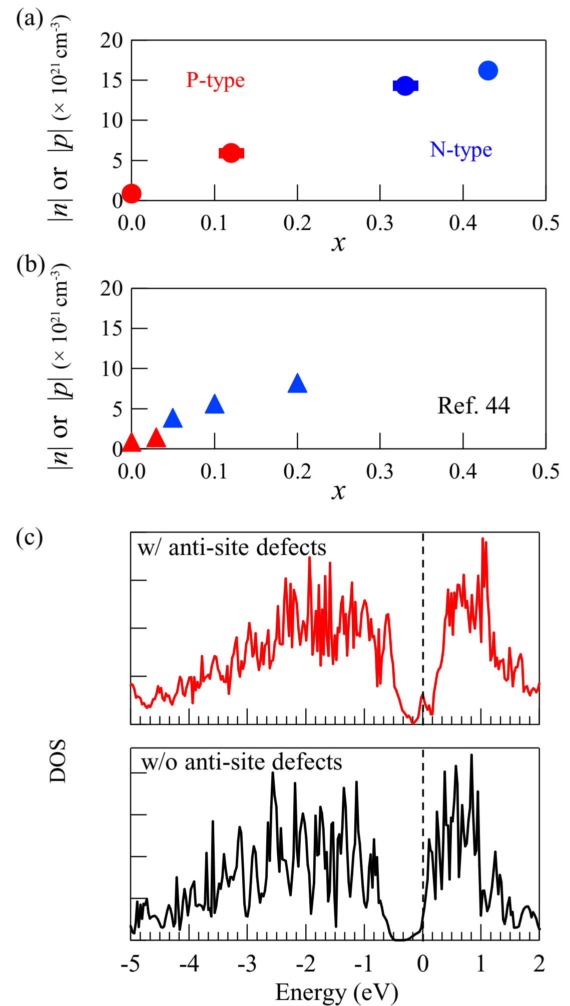

FIG. 4. Absolute value of carrier concentration of the (a) $Fe_2VAl_{1-x}Si_x$ epilayers and (b) polycrystalline $Fe_2VAl_{1-x}Si_x$ bulk [44] at 300 K as a function of x. (c) Total density of states (DOS) of $Fe_2VAl_{0.875}Si_{0.125}$ for V-Si antisite defects (top) and $L2_1$-ordered (bottom) configuration. The dotted vertical lines indicate E_F.

Next, the absolute value of the electron/hole concentration ($|n|$ or $|p|$) versus x for the $Fe_2VAl_{1-x}Si_x$ epilayers and the $Fe_2VAl_{1-x}Si_x$ polycrystalline bulks in Ref. [44] is shown in Figs. 4(a) and 4(b), respectively. Here the value of $|n|$ or $|p|$ in the $Fe_2VAl_{1-x}Si_x$ epilayers was estimated from the slope of the Hall voltage versus applied magnetic field (H) curves in the high magnetic region ($|H| > 7$ T). In Fig. 4(a) the value of $|n|$ or $|p|$ is increased by increasing x (Si substitution) and the carrier polarity is switched from p-type to n-type. Whereas the switching of the carrier polarity at $x = 0.05$ in polycrystalline bulks in Ref. [44] is already observed in Fig. 4(b), it cannot be seen in the $Fe_2VAl_{1-x}Si_x$ epilayers in Fig. 4(a). Namely,

the switching of the carrier polarity was seen at $x = 0.05$ for the polycrystalline bulks [44] while that occurs $x = 0.12$–0.33 for the MBE-grown epilayers. Taking the data in Figs. 1–3 into account, we can guess that the above deviation is derived from the change in the electronic band structure, induced by the decrease in the degree of $L2_1$ ordering in $Fe_2VAl_{1-x}Si_x$ epilayers.

To interpret the electrical properties described above, we conducted first-principles calculations for Si-substituted Fe_2VAl to confirm the impact of the decrease in the degree of $L2_1$ ordering on the electronic band structure, where the electronic band structure calculations for perfect and disordered structures of the Heusler-type Fe_2VAl alloys were performed using the Vienna *ab initio* Simulation Package (VASP) for the pseudopotential method [54–58]. In the calculation, the generalized gradient approximation (GGA) of Perdew, Burke, and Ernzerho was used to express the exchange-correlation potential [59,60], and the projector augmented wave (PAW) potentials were used for describing the valence and core electrons [61,62]. The first Brillouin zone was sampled with a $2 \times 2 \times 2$ k-point mesh. The cutoff and convergence energies were set to 500 and 10^{-5} eV, respectively. The optimized lattice parameter of each structure was determined by the relation between the total energy and lattice parameter fitting to the Birch-Murnghan equation. All calculations were performed using a large-scale parallel computer system in Research Center for Computational Science of Okazaki in Japan.

Because the structural characterizations in Figs. 1 and 2 imply that the Si substitution mainly induces the decrease in the degree of $L2_1$ ordering, the predominant disorder in the $Fe_2VAl_{1-x}Si_x$ epilayers can be regarded as V-Si antisite defects. Thus, we focus on the electronic band structure around E_F for Si-substituted Fe_2VAl with and without the antisite defects. To calculate the effect of the decrease in the degree of $L2_1$ ordering on the electronic band structure, the band structure calculations on the Heusler $Fe_2VAl_{0.875}Si_{0.125}$ ($Fe_{64}V_{32}Al_{28}Si_4$) with and without the V-Si antisite defects were performed. For calculation in the dilute Si substitution system, $2 \times 2 \times 2$ supercells for the Heusler-alloy unit cell ($Fe_8V_4Al_4$) were used. As the part of the unit cell on $L2_1$-ordered Fe_2VAl and $Fe_2VAl_{0.875}Si_{0.125}$ with and without the V-Si antisite defects, we used the crystal structures in Figs. S2(a)–S2(c) in the Supplemental Material [53]. The POSCAR files used for the calculations were also attached to the Supplemental Materials for references. Figure 4(c) shows DOS of $Fe_2VAl_{0.875}Si_{0.125}$ ($x = 0.125$) with (top panel) and without (bottom panel) antisite defects. As described in a previous work [44], for $x = 0.125$ without antisite defects, an evident pseudogap structure around E_F is reconfirmed (bottom panel). As a consequence, the line of E_F is located on the conduction band, leading to the rapid change in the carrier polarity from p-type to n-type [44]. For $Fe_2VAl_{0.875}Si_{0.125}$ with antisite defects, on the other hand, an in-gap state at E_F can be clearly seen (top panel). The presence of the in-gap state at E_F enables to disturb the switching of the carrier polarity, as shown in Fig. 4(b). This scenario is consistent with the presence of a small change in ρ between $x = 0.12$ and 0.22, shown in Fig. 3. From these considerations, the electrical properties in Figs. 3 and 4(a) in the Si-substituted Fe_2VAl epilayers can be interpreted by the impact of the decrease in the degree of $L2_1$ ordering on the electronic band structure.

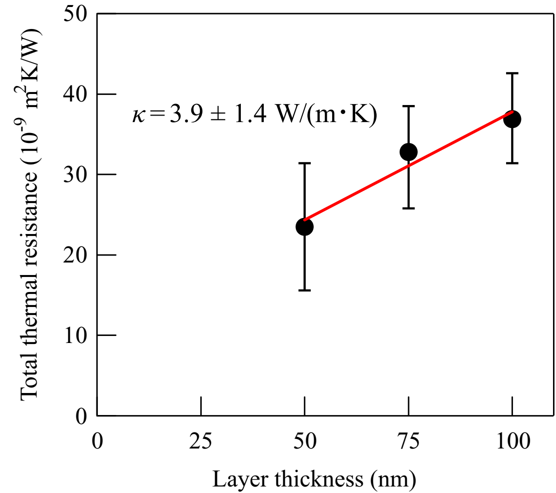

FIG. 5. Total thermal resistance as a function of layer thickness for the $Fe_2VAl_{0.57}Si_{0.43}$ epilayer.

C. Thermoelectric properties

To explore the correlation between the atomic-level disorder in $Fe_2VAl_{1-x}Si_x$ epilayers and thermoelectric properties, we measured the values of the Seebeck coefficient (S) and κ for the $Fe_2VAl_{0.57}Si_{0.43}$ epilayers at 300 K. Here, because the $MgAl_2O_4$ substrate is an insulator with an extremely large sheet resistance ($>10^7$ Ω/sq), the measured S value corresponds to that of the $Fe_2VAl_{0.57}Si_{0.43}$ epilayer with a relatively small sheet resistance of ($\sim 10^2$ Ω/sq). As a result, the value of S is estimated to be $-64 \sim -87$ μV/K, as shown in the Supplemental Material (Fig. S3) [53]. Although the sign of S was changed from positive to negative by substituting Si for Al even in the $Fe_2VAl_{1-x}Si_x$ epilayers, the magnitude of S was relatively low compared to that for bulks (~ 130 μV/K) [44]. Thus, we experimentally judge that there is an impact of the decrease in the degree of $L2_1$ ordering on S values, as discussed in Refs. [63,64].

Next, the cross-plane κ value in the $Fe_2VAl_{0.57}Si_{0.43}$ epilayers was measured using the 2ω method [4,15], where the thermoreflectance signal was fitted by the one-dimensional heat dissipation model using the literature value [65,66]. For measuring a thermal resistance, Au films were deposited on the epilayer surfaces. It should be noted that the sheet resistance of the Au films (0.1–0.7 Ω/sq) was three orders of magnitude smaller than that of the $Fe_2VAl_{0.57}Si_{0.43}$ epilayers ($\geqslant 100$ Ω/sq). Thus, the Joule heating in the $Fe_2VAl_{0.57}Si_{0.43}$ epilayers can be negligible. The details of the measurements for Fe_2VAl epilayers were reported in our previous study [47]. To obtain reliable κ values, we evaluated the layer-thickness dependence of the thermal resistance, as shown in Fig. 5. Because we observe a linear relationship between the thermal resistance and layer thickness, we can assume that the obtained thermal resistance is a series of a layer thermal resistance and an interfacial thermal resistance [47]. According to the reciprocal of the slope, the κ value at 300 K

TABLE I. Comparison of ρ, κ_c, and κ_{ph} at 300 K among this work, Ref. [43], and Ref. [47].

	Epitaxial film (this work) $Fe_2VAl_{0.57}Si_{0.43}$	Epitaxial film [47] Fe_2VAl	Polycrystalline bulk [43] $Fe_2VAl_{0.6}Si_{0.4}$	Polycrystalline bulk [43] Fe_2VAl
Ordering	$L2_1$ (w/ V-Si anti-site defects)	$L2_1$	$L2_1$	$L2_1$
ρ ($\mu\Omega$cm)	4.7×10^2	$\sim 1.4 \times 10^3$	$\sim 2.9 \times 10^2$	$\sim 1.0 \times 10^3$
κ_c [W/(m K)]	∼1.6	∼0.53	∼2.6	∼0.73
κ_{ph} [W/(m K)]	∼2.3	∼7.0	∼11	∼23

can be estimated, as shown in Fig. 5. Note that a low κ value of $\sim 3.9 \pm 1.4$ W/(m K), smaller than bulk and thin-film samples of polycrystalline Fe_2VAl-based alloys with heavy element substitution and/or small grain sizes [10,16], is obtained. The low value of $\sim 3.9 \pm 1.4$ W/(m K) is comparable to that of bulk Ru_2NbGa alloys [~ 5.0 W/(m K)] [67]. Since the κ value did not depend on the layer thickness for the $Fe_2VAl_{0.57}Si_{0.43}$ epilayer, the low κ value was not caused by introducing the low-dimensional structures [64]. Thus, we should discuss the correlation between the decrease in the degree of $L2_1$ ordering in $Fe_2VAl_{1-x}Si_x$ epilayers and the significant reduction in κ later.

We finally comment on the thermoelectric performance of the $Fe_2VAl_{1-x}Si_x$ epilayers. The dimensionless figure of merit [$ZT = S^2T/(\rho\kappa)$] at 300 K for $x = 0.43$ can be estimated to be $0.067 \sim 0.11$, which is lower than the highest ZT value of ∼0.25 (at 300 K) in one of the Fe_2VAl-based alloys, i.e., the $Fe_2VTa_{0.05}Al_{0.95}$ bulk [46]. The low ZT value is attributed to the presence of the in-gap state at E_F, disturbing the enhancement in $|S|$. Thus, we should further study how to simultaneously demonstrate the reduction in κ and the enhancement in $|S|$ even in the epilayers.

III. DISCUSSION

To discuss a possible origin of the low κ value [$\sim 3.9 \pm 1.4$ W/(m K)] for the $Fe_2VAl_{0.57}Si_{0.43}$ epilayer, we summarize the correlation among $L2_1$ ordering, ρ, κ_c, and κ_{ph} in Table I for the $Fe_2VAl_{0.57}Si_{0.43}$ epilayer and $Fe_2VAl_{0.6}Si_{0.4}$ polycrystalline bulks in Ref. [43], together with those for the Fe_2VAl epilayer in Ref. [47] and the Fe_2VAl polycrystalline bulk in Ref. [43]. Here, the value of κ_c was evaluated using the Wiedemann-Franz law, $\kappa_c\rho/T = L_0$, where L_0 is the Lorenz number ($= 2.45 \times 10^{-8}$ WΩK^{-2}) [43,44]. As consequences, the order of the κ_c value in the $Fe_2VAl_{0.57}Si_{0.43}$ epilayer corresponds to that in the $Fe_2VAl_{0.6}Si_{0.4}$ polycrystalline bulk in Ref. [43]. On the other hand, the κ_{ph} value in the $Fe_2VAl_{0.57}Si_{0.43}$ epilayer is about one-fourth of that in the polycrystalline bulk [43]. This feature means that the low total κ of the $Fe_2VAl_{0.57}Si_{0.43}$ epilayer originates mainly from the very low value of κ_{ph} [~ 2.3 W/(m K)] at 300 K. Because the tendency of the decrease in κ_{ph} with substituting Si for Al in the epilayers is similar to that in the polycrystalline bulks in Ref. [43], we can roughly discuss that the phonon scattering is mainly due to the point defects, as discussed in Ref. [43].

Judging from the experimental and theoretical investigations in Figs. 1–4, we can understand that the significant reduction in κ of the Si-substituted Fe_2VAl epilayer in Fig. 5 is given by the decrease in the degree of $L2_1$ ordering, particularly, due to the presence of V-Si antisite defects. Namely, we can regard the very low κ_{ph} in the Si-substituted Fe_2VAl epilayers as a consequence of the presence of V-Si antisite defects in Fe_2VAl-based Heusler alloys.

Recently, the value of κ_{ph} in disordered alloys such as Si_xGe_{1-x} [19] and $PbTe_{1-x}Se_x$ [23] was argued by first-principles calculations. In alloy systems, the effective phonon scattering rate ($\frac{1}{\tau}$) is defined as the sum of a term describing harmonic scattering due to mass disorder ($\frac{1}{\tau_h}$) and a term describing anharmonic scattering ($\frac{1}{\tau_{ah}}$) in the following Matthiessen's rule [19,23], $\frac{1}{\tau} = \frac{1}{\tau_h} + \frac{1}{\tau_{ah}}$. In a previous work on the polycrystalline bulks [43,44], for $\frac{1}{\tau_h}$, the impacts of the mass disorder and the lattice imperfections such as vacancies were regarded as a possible origin of the reduction in the value of κ_{ph} by the Si substitution. From Table I, however, the value of κ_{ph} in the epitaxial layers is further lowered, which is less than one fourth of that in Ref. [43] and is the lowest value in Fe_2VAl-based Heusler alloys. To understand the very low κ_{ph} value, the contribution of $\frac{1}{\tau_{ah}}$ to $\frac{1}{\tau}$ should also be considered in Fe_2VAl-based Heusler alloys as well as half-Heusler alloys [68].

IV. CONCLUSION

We experimentally found that the substitution of Si for Al in Fe_2VAl epilayers markedly affects the reduction in the thermal conductivity. From the measurements of electrical properties and the electronic band structures obtained by the first-principles calculations, we understood that the Si substitution for Al induced the decrease in the degree of $L2_1$ ordering, giving rise to the formation of V-Si antisite defects in the epilayers. For $Fe_2VAl_{0.57}Si_{0.43}$ epilayers, we demonstrated a low thermal conductivity of ∼3.9 W/(m K), one-third less than Si-substituted Fe_2VAl bulk samples [43]. We discussed that a possible origin of the low thermal conductivity is related to the very low lattice thermal conductivity due to the presence of the V-Si antisite defects. We propose that, in addition to the mass disorder effect on the phonon scattering, it is required to consider the impact of the anharmonic scattering in Fe_2VAl-based Heusler alloys with the presence of V-Si antisite defects.

ACKNOWLEDGMENTS

The authors would like to thank Professor T. Taniyama of Tokyo Institute of Technology (the present affiliation is Nagoya University) for providing the opportunity to use an XRD instrument. The computations were performed using Research Center for Computational Science, Okazaki,

Japan. This work was partly supported by Grants-in-Aid for Scientific Research (A) (No. 16H02333 and No. 16H02078), a Grand-in-Aid for Young Scientist (No. 18K13789), and a Fund for the Promotion of Joint International Research (Fostering Joint International Research (B)) (No. 18KK0111) from JSPS. S.Y. acknowledges the support of scholarships from Toyota Physical and Chemical Research Institute Foundation.

[1] G. J. Snyder and E. S. Toberer, Nature Mater. **7**, 105 (2008).
[2] J-F. Li, W.-S. Liu, L.-D. Zhao, and M. Zhou, NPG Asia Mater. **2**, 152 (2010).
[3] X. Zhang and L.-D. Zhao, J. Materiomics **1**, 92 (2015).
[4] Y. Nakamura, Sci. Technol. Adv. Mater. **19**, 31 (2017).
[5] C. Wan, Y. Wang, N. Wang, W. Norimatsu, M. Kusunoki, and K. Koumoto, Sci. Technol. Adv. Mater. **11**, 044306 (2010).
[6] A. Bejan and A. D. Kraus, *Heat Transfer Handbook* (Wiley, New York, 2003), p. 1338.
[7] S. Stackhouse and L. Stixrude, Rev. Mineral. Geochem. **71**, 253 (2010).
[8] J. S. Dugdale and D. K. C. MacDonald, Phys. Rev. **98**, 1751 (1955).
[9] Y. Wang, Y. Sui, J. Cheng, X. Wang, J. Miao, Z. Liu, Z. Qian, and W. Su, J. Alloys Compd. **448**, 1 (2008).
[10] T. Sugiura and Y. Nishino, J. Jpn. Inst. Met. **73**, 846 (2009).
[11] M. Mikami, Y. Kinemuchi, K. Ozaki, Y. Terazawa, and T. Takeuchi, J. Appl. Phys. **111**, 093710 (2012).
[12] T. Takeuchi, Y. Terazawa, Y. Furuta, A. Yamamoto, and M. Mikami, J. Electron. Mater. **42**, 2084 (2013).
[13] W. Kim, J. Zide, A. Gossard, D. Klenov, S. Stemmer, A. Shakouri, and A. Majumdar, Phys. Rev. Lett. **96**, 045901 (2006).
[14] B. Poudel, Q. Hao, Y. Ma, Y. Lan, A. Minnich, B. Yu, X. Yan, D. Wang, A. Muto, D. Vashaee, X. Chen, J. Liu, M. S. Dresselhaus, G. Chen, and Z. Ren, Science **320**, 634 (2008).
[15] Y. Nakamura, M. Isogawa, T. Ueda, S. Yamasaka, H. Matsui, J. Kikkawa, S. Ikeuchi, T. Oyake, T. Hori, J. Shiomi, and A. Sakai, Nano Energy **12**, 845 (2015).
[16] N. Fukatani, Y. Kurosaki, S. Yabuuchi, A. Nishide, and J. Hayakawa, Appl. Phys. Lett. **112**, 033902 (2018).
[17] H. Beyer, J. Nurnus, H. Böttner, A. Lambrecht, E. Wagner, and G. Bauer, Physica E **13**, 965 (2002).
[18] J. C. Caylor, K. Coonley, J. Stuart, T. Colpitts, and R. Venkatasubramanian, Appl. Phys. Lett. **87**, 023105 (2005).
[19] J. Garg, N. Bonini, B. Kozinsky, and N. Marzari, Phys. Rev. Lett. **106**, 045901 (2011).
[20] D. A. Wright, Nature (London) **181**, 834 (1958).
[21] B. Abeles, Phys. Rev. **131**, 1906 (1963).
[22] R. Cheaito, J. C. Duda, T. E. Beechem, K. Hattar, J. F. Ihlefeld, D. L. Medlin, M. A. Rodriguez, M. J. Campion, E. S. Piekos, and P. E. Hopkins, Phys. Rev. Lett. **109**, 195901 (2012).
[23] Z. Tian, J. Garg, K. Esfarjani, T. Shiga, J. Shiomi, and G. Chen, Phys. Rev. B. **85**, 184303 (2012).
[24] Y. Nishino, M. Kato, S. Asano, K. Soda, M. Hayasaki, and U. Mizutani, Phys. Rev. Lett. **79**, 1909 (1997).
[25] G. A. Botton, Y. Nishino, and C. J. Humphreys, Intermetallics **8**, 1209 (2000).
[26] D. J. Singh and I. I. Mazin, Phys. Rev. B **57**, 14352 (1998).
[27] R. Weht and W. E. Pickett, Phys. Rev. B **58**, 6855 (1998).
[28] M. Weinert and R. E. Watson, Phys. Rev. B **58**, 9732 (1998).
[29] A. Bansil, S. Kaprzyk, P. E. Mijnarends, and J. Toboła, Phys. Rev. B **60**, 13396 (1999).
[30] S. Bandaru and P. Jund, Phys. Status Solidi B **254**, 1600441 (2017).
[31] G. Y. Guo, G. A. Botton, and Y. Nishino, J. Phys.: Condens. Matter **10**, L119 (1998).
[32] Y. Nishino, Mater. Trans. **42**, 902 (2001).
[33] H. Okamura, J. Kawahara, T. Nanba, S. Kimura, K. Soda, U. Mizutani, Y. Nishino, M. Kato, I. Shimoyama, H. Miura, K. Fukui, K. Nakagawa, H. Nakagawa, and T. Kinoshita, Phys. Rev. Lett. **84**, 3674 (2000).
[34] C. S. Lue and Joseph H. Ross, Jr., Phys. Rev. B **61**, 9863 (2000).
[35] K. Soda, T. Mizutani, O. Yoshimoto, S. Yagi, U. Mizutani, H. Sumi, Y. Nishino, Y. Yamada, T. Yokoya, S. Shin, A. Sekiyama, and S. Suga, J. Synchrotron Rad. **9**, 233 (2002).
[36] N. F. Mott and H. Jones, *The Theory of the Properties of Metals* (Clarendon Press, Oxford, 1936).
[37] C. S. Lue and Y.-K. Kuo, Phys. Rev. B **66**, 085121 (2002).
[38] M. Mikami, M. Inukai, H. Miyazaki, and Y. Nishino, J. Electron. Mater. **45**, 1284 (2016).
[39] Y. Nishino, H. Kato, M. Kato, and U. Mizutani, Phys. Rev. B **63**, 233303 (2001).
[40] H. Miyazaki, S. Tanaka, N. Ide, K. Soda, and Y. Nishino, Mater. Res. Express. **1**, 015901 (2014).
[41] Y. Nishino and Y. Tamada, J. Appl. Phys. **115**, 123707 (2014).
[42] K. Renard, A. Mori, Y. Yamada, S. Tanaka, H. Miyazaki, and Y. Nishino, J. Appl. Phys. **115**, 033707 (2014).
[43] C. S. Lue, C. F. Chen, J. Y. Lin, Y. T. Yu, and Y. K. Kuo, Phys. Rev. B **75**, 064204 (2007).
[44] Y. Nishino, S. Deguchi, and U. Mizutani, Phys. Rev. B **74**, 115115 (2006).
[45] M. Vasundhara, V. Srinivas, and V. V. Rao, Phys. Rev. B **77**, 224415 (2008).
[46] S. Masuda, K. Tsuchiya, J. Qiang, H. Miyazaki, and Y. Nishino, J. Appl. Phys. **124**, 035106 (2018).
[47] S. Yamada, K. Kudo, R. Okuhata, J. Chikada, Y. Nakamura, and K. Hamaya, Appl. Phys. Express **10**, 115802 (2017).
[48] K. Hamaya, H. Itoh, O. Nakatsuka, K. Ueda, K. Yamamoto, M. Itakura, T. Taniyama, T. Ono, and M. Miyao, Phys. Rev. Lett. **102**, 137204 (2009).
[49] S. Yamada, K. Tanikawa, S. Oki, M. Kawano, M. Miyao, and K. Hamaya, Appl. Phys. Lett. **105**, 071601 (2014).
[50] Y. Fujita, M. Yamada, M. Tsukahara, T. Oka, S. Yamada, T. Kanashima, K. Sawano, and K. Hamaya, Phys. Rev. Applied **8**, 014007 (2017).
[51] K. Arima, F. Kuroda, S. Yamada, T. Fukushima, T. Oguchi, and K. Hamaya, Phys. Rev. B **97**, 054427 (2018).
[52] K. Kudo, S. Yamada, J. Chikada, Y. Shimanuki, Y. Nakamura, and K. Hamaya, Jpn. J. Appl. Phys. **57**, 040306 (2018).
[53] See Supplemental Material at http://link.aps.org/supplemental/10.1103/PhysRevB.99.054201 for the electrical and thermoelectric properties of the $Fe_2VAl_{1-x}Si_x$ films.
[54] G. Kresse and J. Hafner, Phys. Rev. B **47**, 558(R) (1993).
[55] G. Kresse and J. Hafner, Phys. Rev. B **48**, 13115 (1993).
[56] G. Kresse and J. Hafner, Phys. Rev. B **49**, 14251 (1994).

[57] G. Kresse and J. Furthmüller, Comput. Mater. Sci. **6**, 15 (1996).
[58] G. Kresse and J. Furthmüller, Phys. Rev. B **54**, 11169 (1996).
[59] J. P. Perdew, K. Burke, and M. Ernzerhof, Phys. Rev. Lett. **77**, 3865 (1996).
[60] J. P. Perdew, K. Burke, and M. Ernzerhof, Phys. Rev. Lett. **78**, 1396 (1997).
[61] P. E. Blöchl, Phys. Rev. B **50**, 17953 (1994).
[62] G. Kresse and D. Joubert, Phys. Rev. B **59**, 1758 (1999).
[63] S. Hiroi, M. Mikami, and T. Takeuchi, Mater. Trans. **57**, 1628 (2016).
[64] Y. Furuta, K. Kato, T. Miyawaki, H. Asano, and T. Takeuchi, J. Electron. Mater. **43**, 2157 (2014).
[65] St. Burghartz and B. Schulz, J. Nucl. Mater. **212-215**, 1065 (1994).
[66] Y. Kawaharada, K. Kurosaki, and S. Yamanaka, J. Alloy. Compd. **352**, 48 (2003).
[67] C. N. Kuo, H. W. Lee, C.-M. Wei, Y. H. Lin, Y. K. Kuo, and C. S. Lue, Phys. Rev. B **94**, 205116 (2016).
[68] J. Shiomi, K. Esfarjani, and G. Chen, Phys. Rev. B **84**, 104302 (2011).